

Cavity Beam Position Monitors

Ronald Lorenz

DESY Zeuthen, Platanenallee 6, D-15738 Zeuthen

Abstract. Beam-based alignment and feedback systems are essential for the operation of future linear colliders and free electron lasers. A certain number of beam position monitors with a resolution in the submicron range are needed at selected locations. Most beam position monitors detect the electric or the magnetic field excited by a beam of charged particles at different locations around the beam pipe. In resonant monitors, however, the excitation of special field configurations by an off-center beam is detected. These structures offer a large signal per micron displacement. This paper is an attempt to summarize the fundamental characteristics of resonant monitors, their advantages and shortcomings. Emphasis will be on the design of cylindrical cavities, in particular on the estimation of expected signals, of resolution limits and the resulting beam distortion. This includes also a short introduction into numerical methods. Fabrication, tuning, and other practical problems will be reviewed briefly. Finally, some resonant devices used for beam position diagnostics will be discussed and listed.

INTRODUCTION

A linear collider with a center of mass energy of 500 GeV could be used for detailed studies of the top quark system, for finding or excluding the Higgs boson and for the search of supersymmetric particles. Because a luminosity of about $10^{33} \text{ cm}^{-2}\text{s}^{-1}$ is needed due to the small cross sections of the processes of interest, all linear collider studies worldwide consider flat colliding beams having vertical dimensions of 3–20 nm [16]. Beam-based alignment and correction schemes have to be adopted to bring these tiny beams into collision. A certain number of high-resolution beam position monitors (BPM) are needed at selected locations.

Free electron lasers (FEL) are under design [23] for which the power and the coherency of the radiation can be enhanced due to the bunching by emitted radiation in the first part of the undulator, a process known as self-amplified spontaneous emission. Very small beam emittances are essential to reach saturation within a reasonable undulator length. The position of the electron beam might vary inside the undulator, mainly because of field imperfections of the magnets. Since a precise overlap of electron and photon beams is essential for FEL operation, the position of the electron beam has to be measured with a high resolution and corrected along the undulator beamline.

A BPM system consists of a ‘transducer’ close to the beam, transmission lines, electronics, and software. This paper concentrates mainly on the transducer. If a bunch of charged particles is centered in a circular, conducting beam pipe, then there is a uniformly distributed electro-magnetic field accompanying the beam. Its spectrum depends on the bunchlength σ_z , the bunch shape, and the spacing between two bunches. For a ‘short’ bunch spacing and processes having ‘long’ time constants, the spectrum contains discrete lines at harmonics of the bunching frequency. The fields of an off-center beam are not uniformly distributed. Many transducers used in BPM systems detect the electric or the magnetic field at different locations around the beam pipe. These signals are subtracted in the electronics or in a computer to measure the ‘field distortion’ [19].

In resonant cavities the beam excites special field configurations resonating at a certain frequency. The amplitude of these *modes* depends on the cavity orientation, the bunch charge, the beam position, and its spectrum.

Dipole modes are used for position detection, since their amplitude depends linearly on the beam position and is zero for a centered beam. The signals excited in the cavity are coupled into an external circuit, and the amplitude of this particular mode can be separated in the frequency domain. In principle, no additional subtraction is needed, the information about the position is given directly. Because of the large signal per micron displacement, these resonant monitors find application in situations where the beam signals are weak. This paper is an attempt to discuss the characteristics of cavity BPMs, and to summarize their advantages and the trade-offs. Emphasis will be on the design of circular cavities, including the expected signals and some numerical methods.

WAVEGUIDES AND CAVITIES

A waveguide can support waves of any frequency (above cut-off), the guide wavelength taking a value which causes the field patterns to satisfy the boundary conditions. These field patterns can be divided into two basic sets of solutions or modes: ‘transverse magnetic’ or TM modes (no longitudinal magnetic field component) and ‘transverse electric’ or TE modes (no longitudinal electric field component).

The field components of the TM modes in a cylindrical waveguide can be derived from a Hertzian potential having a single component along the axis of the guide [5]. A *generating function* ψ_e , which satisfies the two-dimensional Helmholtz-equation, is then used to calculate these field components:

$$\mathbf{E}_t = \pm\Gamma\nabla_t\psi_e e^{(\pm\Gamma z)} \quad E_z = -\nabla_t^2\psi_e e^{(\pm\Gamma z)} \quad \mathbf{H}_t = \mp\frac{j\mu_0\varepsilon_0\omega^2}{Z_0\Gamma}\mathbf{a}_z \times \mathbf{E}_t \quad (1)$$

where k_c is the cut-off wave number, $\Gamma = k_c^2 - (\omega^2\mu_0\varepsilon_0)$ the propagation constant and $Z_0 = \sqrt{\mu_0/\varepsilon_0}$ the intrinsic impedance of free space. Usually, a solution of the form $\psi_e = U(u_1)U(u_2)$ may be found, where the functions U_1, U_2 depend on the

geometry used. The allowed values of k_c^2 and Γ^2 are determined by the boundary conditions (E_z and \mathbf{H}_t must vanish on the boundary for perfectly conducting walls). At a wavelength λ longer than the cut-off wavelength $\lambda_{c,mn}$ of the mn th mode the fields at a point z_0 from a source are attenuated by

$$\delta_{z_0} = \exp\left(-2\pi \cdot z_0 \cdot \sqrt{\lambda^{-2} - \lambda_{c,mn}^{-2}}\right) \quad \lambda_{c,mn} = 2\pi \cdot (k_{c,mn})^{-1} \quad (2)$$

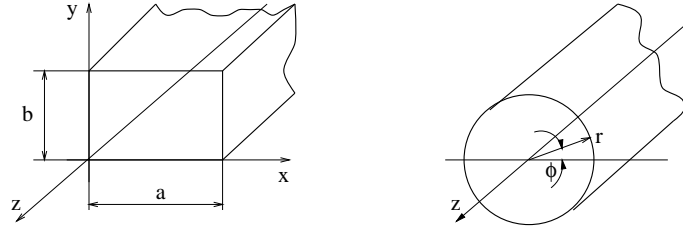


FIGURE 1. Coordinate systems for rectangular and for circular waveguides.

Rectangular Waveguides

Following the coordinate system in Figure 1, the field generating functions of the TM modes and the cut-off wave numbers of rectangular waveguides are given [5] by

$$\psi_{nm} = \cos\left(\frac{n\pi x}{a}\right) \cdot \sin\left(\frac{m\pi y}{b}\right) \quad k_{c,nm} = \left(\frac{n\pi}{a}\right)^2 + \left(\frac{m\pi}{b}\right)^2. \quad (3)$$

Circular waveguides

Using Figure 1, the field generating functions of the TM modes and the cut-off wave numbers of circular waveguides are given [5] by

$$\psi_{mn} = J_m(k_{c,mn}) \cdot \cos(m\phi) \quad k_{c,mn} = \frac{a_{mn}}{r} \quad (4)$$

where a_{mn} is the n -th zero of the Bessel function J_m .

Resonant Cavities

If a waveguide is closed by two short-circuiting planes, boundary conditions will have to be met on these planes. This requires the planes to be separated by an integral number of half-wavelengths, and waves can be excited in the enclosure only at discrete frequencies. Such a resonating enclosure is called a *cavity* (but a cavity is not necessarily a waveguide section). In the following the indices for the different modes are neglected, where appropriate. For a more detailed discussion the reader is referred to [5].

Cavities — Equivalent Circuits

The energy in a cavity oscillates between pure electric and pure magnetic energy; the averaged stored electromagnetic energy is $W_s = \langle W_e \rangle + \langle W_m \rangle = 2 \cdot \langle W_e \rangle$. For a certain mode, this is equivalent to a circuit containing a capacitor and an inductor.¹ In an equivalent circuit for the whole cavity, there are many LC-circuits in parallel. Three cavity quantities that are independent of the field strength are needed to calculate the parameters R , L , and C for each mode. The resonance frequency is given by $\omega_r = (L \cdot C)^{-\frac{1}{2}}$. The definition for the shunt impedance following the circuit theory is

$$R = \frac{\left| \int_0^t E_z \cdot e^{j\omega t} dz \right|^2}{2P_d} = \frac{|V_{mn0}|^2}{2P_d}. \quad (5)$$

The integral in the numerator depends not only on the cavity shape and the chosen mode, but also on the integration path (here, the particle trajectory).

Practical cavities, made of metal, dissipate energy in their walls. In a cavity without any external coupling (free oscillation), the negative change in time of the stored energy is equal to the dissipated power P_d .

$$-\frac{dW_s}{dt} = P_d \quad \Rightarrow \quad W_s = W_0 \cdot \exp\left(-\frac{\omega_r}{Q_0}t\right) \quad \text{with} \quad Q_0 = \frac{\omega_r W_s}{P_d} = \frac{\omega_r \tau_r}{2} \quad (6)$$

Q_0 is the quality factor of the cavity and is independent of the field strength. Together with ω_r , it determines the decay time τ_r of the cavity.

Coupling to External Circuits

A cavity has also connections to the outer world, for feeding or to couple out the signals (e.g., for measurements). Such a connection can be realized by

1. Magnetic coupling, where the H-field passes through a loop and induces a voltage (as shown in Fig. 2a),
2. Electric coupling, where the E-field causes a current on a small dipole (Fig. 2c), and
3. Electromagnetic coupling by an aperture, where electric and magnetic fields penetrate through a hole in the common wall, corresponding to an electric dipole or magnetic dipoles in an external waveguide (Fig. 2b and 2d).

By choosing the antenna length, the form of the loop, and its position correctly the coupling factor β can be adjusted. The coupling is also explained in terms of the *external Q value* Q_{ext} and the *loaded Q* Q_L

$$Q_L = (Q_0 \cdot Q_{\text{ext}}) / (Q_0 + Q_{\text{ext}}) = Q_0 / (1 + \beta) \quad \text{with} \quad \beta = P_{\text{out}} / P_d. \quad (7)$$

1. Note: In real cavities, both energies are not concentrated in lumped elements!

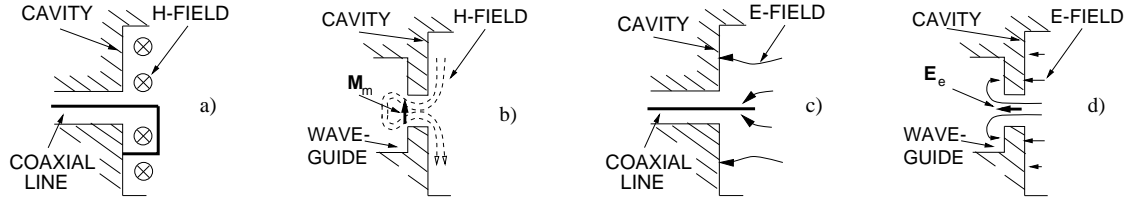


FIGURE 2. Magnetic coupling by a) a loop and b) through a hole; electric coupling by c) an antenna and d) through a hole.

Cavities in Particle Accelerators

Coupling to a Beam

One of the most common applications of a cavity in particle accelerators is the use as the source of the accelerating rf voltage. A charge q passing an empty cavity leaves a field behind it that can be represented by an infinite sum of modes (Fourier series). Each mode n can be described by ω_n , Q_n and the instantaneous voltage V_n along the particle path. The stored energy W_n in this mode will be proportional to the square of the charge. A fraction U_n of the total energy, the particle has lost, is radiated in mode n . It can be expressed by a decelerating voltage proportional to the induced voltage V_n . The statement that a charge passing a cavity sees exactly one-half of its own induced voltage (remaining after the passage) is called the *fundamental theorem of beam loading*. By conservation of energy, the stored energy in mode n must be equal to the energy radiated into this mode. Using Equation (5) one gets for V_n and for the *loss factor* k_n

$$V_n = 2 \cdot q \cdot k_n \quad \text{with} \quad k_n = \frac{V_n^2}{4 \cdot W_n} = \frac{\omega_n}{2} \cdot \left(\frac{R}{Q} \right)_n. \quad (8)$$

If we want the voltage V_n to be the actual voltage excited by the bunch in the cavity we have to take into account the change of the E-field during the passage time. Often this phase difference between the particle beam and the rf field is called the *transit time factor*. For a velocity of $v = c_0$ one finds

$$T_{tr} = \left(\int_{z_1}^{z_2} E_z \cdot e^{jkz} \cdot dz \right) / \left(\int_{z_1}^{z_2} E_z \cdot dz \right) = \frac{\sin \eta}{\eta} \quad \text{with} \quad \eta = \frac{\pi \cdot l}{\lambda_{mn0}}. \quad (9)$$

Tuning of a Cavity

High-Q cavities having a small bandwidth can be detuned by small temperature changes. Fabrication tolerances and temperature drifts have to be tuned out for most applications to be exactly on resonance. Since the adjustment of an external impedance would also change the coupling, tuning is often done by deformations of the inner cavity surface ('screws'). This can be done in regions of high

- E-field by changing the length s of an E-field trajectory, corresponding to a change of the capacitance

$$(C + \Delta C) = \frac{Q}{E(s + \Delta s)}.$$

- H-field by changing the area A where the magnetic flux passes through (changes the inductance)

$$(L + \Delta L) = \frac{\mu H}{I} (A + \Delta A).$$

Both result in a new resonance frequency $\omega_r + \Delta\omega_r = [(L + \Delta L)(C + \Delta C)]^{-\frac{1}{2}}$.

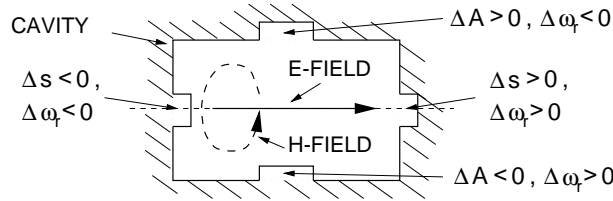


FIGURE 3. Tuning of cavity by changing the inner surface.

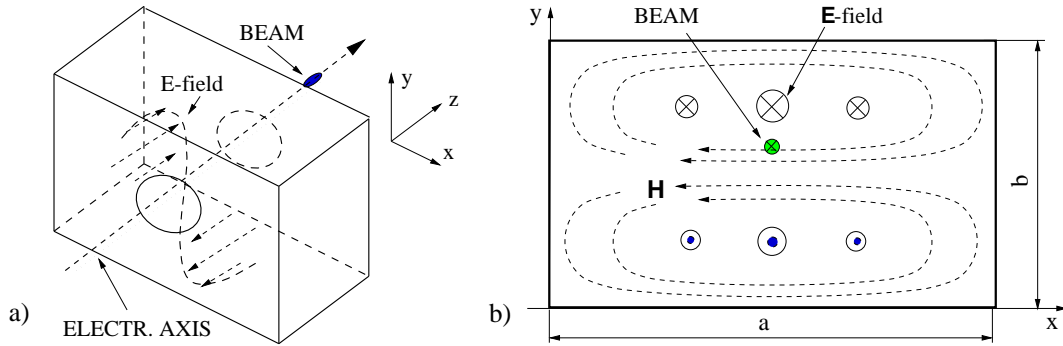


FIGURE 4. a) Beam-excited rectangular cavity; b) field pattern of the TM_{120} mode.

Example 1: Rectangular Cavities used as BPMs at SLAC.

Resonant monitors using rectangular cavities excited in the TM_{120} mode were built at SLAC many years ago [9]. The longitudinal E-field component of this mode and its resonant frequency are given by

$$E_z(x, y) = E_z^{max} \cdot \sin(\pi x/a) \cdot \sin(2\pi y/b) \quad f_{120} = c_0/2 \cdot \sqrt{(1/a)^2 + (2/b)^2}. \quad (10)$$

The cavities were fabricated from OFHC copper plates and brazed. A resolution of 10 μm was reached for a beam current of about 100 μA by using a homodyne detection system. The cavity output power was about 50 $\mu\text{W}/(\text{mA}^2\text{mm}^2)$.

CIRCULAR CAVITIES

The simplest microwave BPM structure is a circular cavity excited in the TM_{110} mode by an off-axis beam. The amplitude of this mode yields a signal proportional to the beam displacement and the bunch charge; its phase relative to an external reference gives the sign of the displacement. This signal is much stronger than the signal given by other monitors and is a linear function of the beam displacement.

Fields and Signals of the TM_{110} Mode

First, only unperturbed cavities are considered and the influence of the beam pipe and of coupling ports are neglected. The resonant frequency and the z-component of the $mn0$ th TM mode electric field at a position δx are given by

$$E_{mn0} = C_{mn0} \cdot J_m \left(\frac{a_{mn}\delta x}{R_{\text{res}}} \right) \cdot \cos(m\phi) \cdot e^{-(j\omega z)} \quad f_{mn0} = \frac{c_0 \cdot a_{mn}}{2\pi \cdot R_{\text{res}}} \quad (11)$$

(r, ϕ, z) is the position in cylindrical coordinates, t the time, and C_{mn0} the amplitude. The electric and magnetic fields of the first dipole mode are shown in Figure 5b. The Q value of this TM_{110} mode and the R/Q at the position [$r_{E_{\text{max}}} = 0.481 \cdot R_{\text{res}}$] of its electrical field maximum are given by

$$Q_{110} = \frac{1}{2\pi} \cdot \frac{a_{11}}{1 + (R_{\text{res}} \cdot l^{-1})} \cdot \frac{\lambda_{110}}{\delta} \quad \text{with} \quad \delta = \sqrt{\frac{1}{\pi \cdot f_{110} \cdot \mu \cdot \kappa}} \quad (12a)$$

$$\left(\frac{R}{Q} \right)_{110} = \frac{(V_{110}^{\text{max}})^2}{2\omega_{110} \cdot W_{110}} = \frac{2 \cdot Z_0 \cdot l \cdot (J_1^{\text{max}})^2 \cdot T_{tr}^2}{\pi \cdot R_{\text{res}} \cdot J_0^2(a_{11}) \cdot a_{11}} \approx 130.73 \cdot \frac{l}{R_{\text{res}}} \cdot T_{tr}^2 \quad (12b)$$

where a_{11} is the first root of J_1 , $J_1^{\text{max}} = J_1(1.841) = 0.582$ at its maximum.

Beam-Excited TM_{110} Signals

The voltage V_{110}^{in} induced in the TM_{110} mode by a charge q at $(\delta x, \phi = 90^\circ)$ can be calculated by using Equation (11) and the maximum voltage. $V_{110}(r_{E_{\text{max}}})$ can be expressed in terms of the loss factor k_{110} and the bunch charge q (Eqn. (8)).

$$\frac{V_{110}^{\text{in}}(\delta x)}{V_{110}(r_{E_{\text{max}}})} = \frac{J_1 \left(\frac{a_{11}\delta x}{R_{\text{res}}} \right)}{J_1^{\text{max}}} \quad \Rightarrow \quad V_{110}^{\text{in}}(\delta x) = \frac{2 \cdot k_{110} \cdot q}{J_1^{\text{max}}} \cdot \frac{a_{11} \cdot \delta x}{2 \cdot R_{\text{res}}} \quad (13)$$

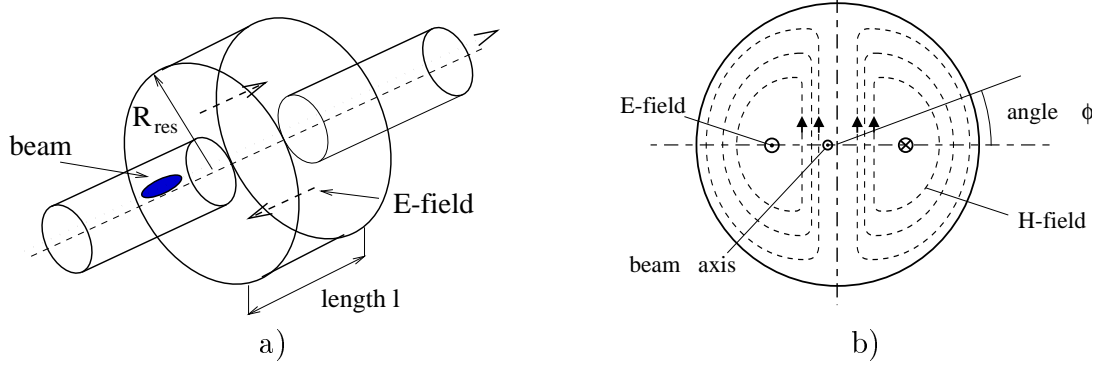


FIGURE 5. a) Beam-excited TM_{110} in a circular cavity; b) fields of the horizontal polarization.

The Bessel function $J_1(x)$ can be replaced by $x/2$ for small arguments,² and the voltage becomes linear proportional to δx . Together with Equation (12b) this gives

$$V_{110}^{in}(\delta x) = \left(\frac{R}{Q}\right)_{110} \cdot \omega \cdot q \cdot \left\langle \frac{a_{11} \cdot \delta x}{2 \cdot J_1^{max} \cdot R_{res}} \right\rangle = \delta x \cdot q \cdot \frac{l \cdot T_{tr}^2}{R_{res}^3} \cdot 0.2474 \left[\frac{\text{Vm}}{\text{pC}} \right]. \quad (14)$$

The term in the angle brackets is also called the *beam coupling coefficient*, M_b .

In the case of a cavity excitation by *multiple bunches* the cavity has to reach its steady state and an averaged position of the bunch train will be measured. With the length of the bunch train, τ_s , and with τ_r (Eqn. (6)) this results in $Q_L \ll \omega \tau_s$. The power coupled out of the cavity and the voltage into a $50\text{-}\Omega$ system can be estimated using the averaged beam current $\langle I_b \rangle = 2 \cdot I_{DC}$.

$$P_{out} = \left(\frac{R}{Q}\right)_{110} \cdot Q_L \cdot \langle I_b \rangle^2 \cdot M_b^2 \cdot \frac{\beta}{1 + \beta} \quad V_{110}^{out} = \sqrt{P_{out} \cdot 50 \text{ }\Omega}. \quad (15)$$

When a *single bunch* traverses the cavity it will excite a burst of rf that decays with τ_r . A proper Q_L has to be chosen so that the cavity is ‘empty’ when the next bunch comes (see also Eqn. (6)).

$$V_{110}(t_b) = V_{110}(t=0) \cdot \exp\left(-\frac{1}{2} \cdot t_b \cdot \frac{\omega_{110}}{Q_L}\right) = \exp\left(-\frac{1}{2} \cdot \frac{t_b}{t_{r,l}}\right) \quad (16)$$

The rf current during such a burst will be $I_{rf} = q \cdot \tau_{r,l}/2$. With Equation (15) we get for the voltage excited by a single bunch and coupled into a $50\text{-}\Omega$ system.

$$V_{110}^{out}(\delta x) = \left(\frac{R}{Q}\right) \omega q \sqrt{\frac{50 \text{ }\Omega}{Q_L}} M_b \frac{\beta}{1 + \beta} = V_{110}^{in}(\delta x) \left(\frac{R}{Q}\right)_{110}^{-\frac{1}{2}} \sqrt{\frac{50 \text{ }\Omega}{Q_L}} \sqrt{1 - \frac{Q_L}{Q_0}} \quad (17)$$

2. The error of this relation is less than 1% up to $\delta x = 0.14 \cdot R_{res}$.

Other Signals and Resolution Limits

Common-Mode Signals

Since the field maximum of the common modes is on the cavity axis, they will be excited much stronger than the TM_{110} by a beam near the axis. The excitation of the dominant TM_{010} mode at its own frequency can be estimated following [17]:

$$S_1 = \frac{V_{110}(\omega_{110})}{V_{010}(\omega_{010})} = \frac{1}{J_1^{\max}} \frac{\delta x \cdot a_{11}}{2 \cdot R_{\text{res}}} \cdot \frac{V_{110}^{\max}}{V_{010}} \approx \frac{5.4}{\lambda_{110}} \cdot \delta x \cdot \frac{k_{110}}{k_{010}}. \quad (18)$$

This gives the frequency-sensitive TM_{010} rejection, which has to be realized mainly in a band-pass filter. Assuming that both loss factors are identical, 69 dB rejection are required to detect a beam displacement of 10 μm in a 1.52-GHz cavity.

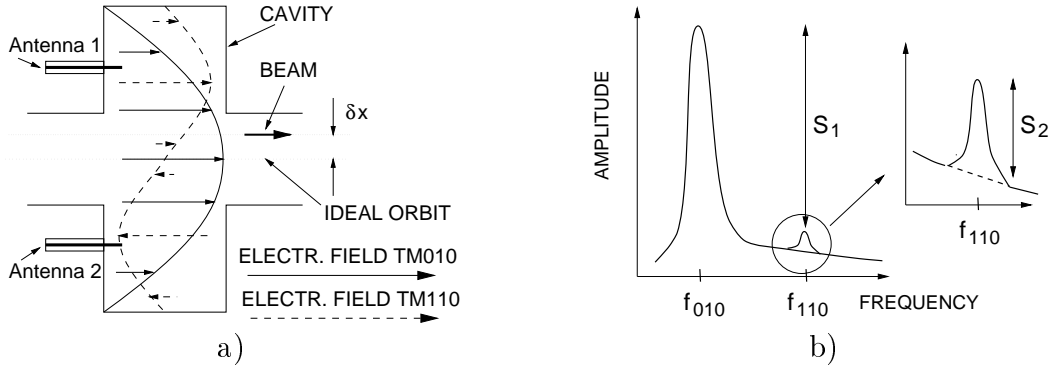


FIGURE 6. a) Excitation of the TM_{010} and the TM_{110} ; b) signals in the frequency domain.

Due to their finite Q , all modes have field components even at the TM_{110} -mode frequency as sketched in Figure 6. The ratio of the spectral densities at ω_{110} was estimated in [17], leading to a position δx^{\min} close to the electrical center where both signals are identical (smaller displacements can not be detected):

$$S_2 = \frac{v_{110}(\omega_{110})}{v_{010}(\omega_{110})} \approx S_1 \cdot Q_L \cdot \left(1 - \frac{\omega_{010}^2}{\omega_{110}^2}\right) \Rightarrow \delta x^{\min} \approx \frac{k_{010}}{k_{110}} \cdot \frac{R_{\text{res}}}{2 \cdot Q_L} \quad (19)$$

This pessimistic estimation assumes a cw-excitation and a detection scheme which is not sensitive to the phase difference between the two voltages.

Effect of Beam Angle

Let us assume a beam, that goes through the cavity center with an angle x' . By integrating the E-field along this new particle trajectory, we get [14]

$$T_{tr} \cdot M_b = \frac{a_{11}^2 \cdot l^2 \cdot x'}{12 \cdot J_1(\rho_{01}) \cdot R_{\text{res}}^2} = 2.36 \frac{l^2 \cdot x'}{R_{\text{res}}^2} \quad V_{110}(x') \simeq j \cdot A_3 \cdot q \cdot x'. \quad (20)$$

Together with Equation (14) we get an offset error of

$$\frac{\delta x}{x'} = \frac{2244.5}{\sin(\pi l \cdot \lambda^{-1})} \cdot \frac{l^3}{R_{\text{res}}^2} \cdot \frac{1}{\lambda} \left[\frac{\text{m}}{\text{mrad}} \right] \quad (21)$$

Summary — Resolution Limits and Conclusions

As shown above, the cavity output signal at the frequency ω_{110} contains also other signals than a ‘clean’ TM_{110} voltage. This is summarized in Equation (22) (the A_n are constants) and illustrated in the right part of Figure 7b:

$$V_{\text{cav}}(\omega_{110}) = V_{110}^{\text{out}}(\delta x) + V_{0n0} + V_{110}(x') + V_n = A_1 q x + j A_2 q + j A_3 q x' + V_n. \quad (22)$$

The second term is caused by the common-mode leakage, the third term displays the beam angle, and the last one is the electronics noise.

Considering two opposing antennae (1 and 2 in the cavity of Fig. 6a), the TM_{010} and the TM_{110} fields have a phase difference of 180° . If these signals are combined in a hybrid or a Magic-T, the TM_{110} signal appears at the Δ -port. This effect is also sketched in Figure 11 (frequency domain). The rejection of common-mode components in such a field-selective filter — and thus the improvement of the ‘center resolution’ — is limited by the isolation between the Σ - and the Δ -port of the device used. Standard hybrids have an isolation of about 25 dB. Furthermore, the beam-angle signal and the common-mode signal are phase shifted by $\pi/2$ and can be suppressed by using a synchronous detector. If the remaining phase error in the system is very small, the resolution is mainly limited by the electronics noise.

Example 2: Cavity-BPMs installed at the Final Focus Test Beam (FFTB)

Often the amplitude of the beam position jitter is in the order of some microns and it is impossible to predict the beam trajectories. But at high energies the trajectories are ‘straight’ lines, and three BPMs can be used to measure their intrinsic resolution. A block of three C-band TM_{110} cavities was tested at the FFTB at SLAC [14], and the measured resolution was about 25 nm (Fig. 8b).

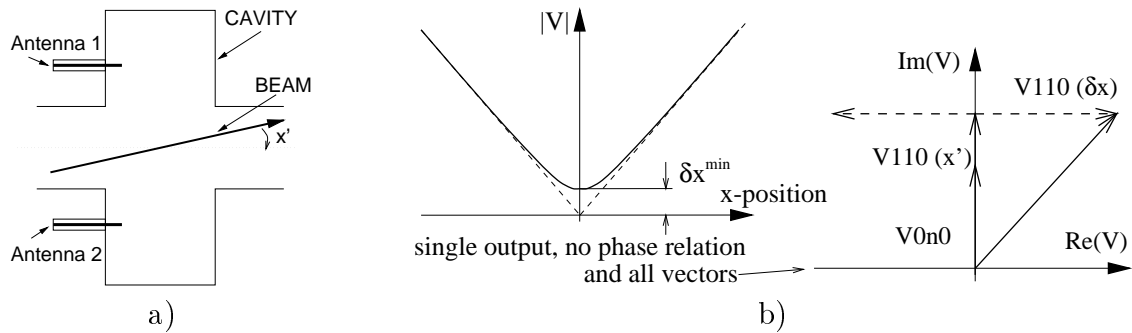


FIGURE 7. a) Effect of a beam angle; b) signals excited in the cavity (summary).

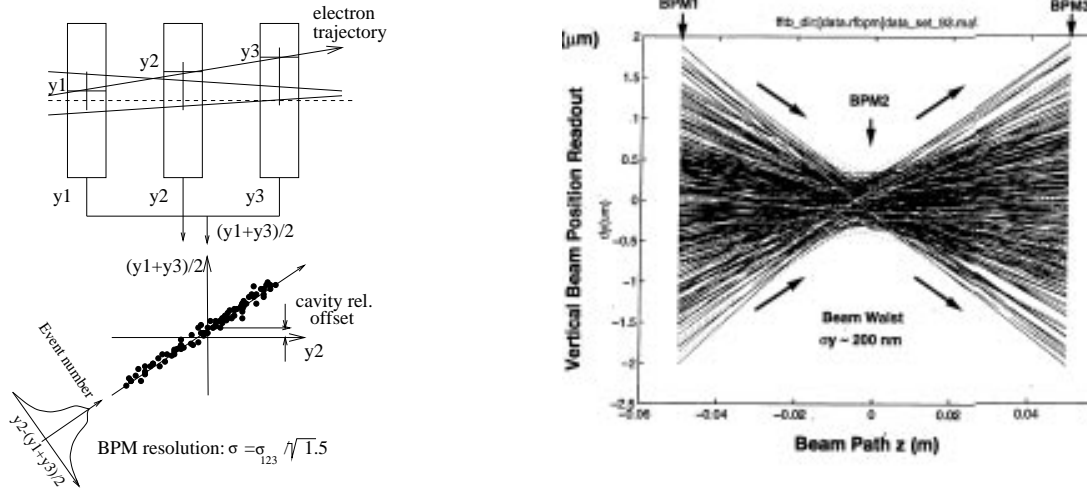


FIGURE 8. a) Resolution measurements at the FFTB using three cavities; b) pulse-to-pulse multiple beam trajectory traces [19].

Wakefields

Since a charged particle interacts electromagnetically with the surroundings (e.g., discontinuities in a metallic vacuum chamber), it generates an electromagnetic field. This so-called *wakefield* acts back on the motion of following particles within the same bunch or even within other bunches, leading to deflection or deceleration. The *wake potentials* are obtained by integrating the longitudinal or transverse components of the Lorentz force at a distance s behind the exciting charge moving on a straight path with constant velocity. The form of these potentials depends on the structure and on the bunch length.

Since impedances are also the Fourier transforms of the delta-function wake, there is a strong correlation between the signals coupled out of a structure (‘pick-up’ of any geometry) and the wakefield. Therefore, the high shunt impedance of a cavity BPM causes problems for many circular machines such as storage rings and light sources. Usually, the number of such devices adding a remarkable amount to the impedance budget has to be minimized.

An analytical approach for the wakefield of a cavity gap and very short bunches is the *diffraction model* [3]. It can be used to estimate the peak wake potential of a cavity of length g having an entrance aperture of radius R_0 , and a Gaussian bunch with a rms length σ_z :

$$\hat{W}_{diff} = \frac{Z_0 c}{\sqrt{2\pi^2 R_0}} \sqrt{\frac{g}{\sigma_z}} = 8.1 \cdot \frac{1}{R_0} \cdot \sqrt{\frac{g}{\sigma_z}} \quad (\text{in units of } \frac{\text{V}}{\text{nC}}). \quad (23)$$

In most practical cases, the wake potentials must be calculated using computer codes. 2D codes such as ABCI [1] can be used for circular cavities if the effect of a coupling device is negligible. For more complex structures one has to use 3D codes

such as MAFIA. The total loss factor k_{all} (all excited modes of a certain azimuthal symmetry) gives also the *power deposited* in the cavity, P_l :

$$P_l = k_{all} \cdot f_{av} \cdot q^2 \quad \text{with} \quad f_{av} = N_{bunches} \cdot f_{rep}. \quad (24)$$

Example 3: Diagnostic stations for the TESLA Test Facility Linac-FEL

Circular cavities were chosen for this purpose [13] because of the required single bunch resolution of $1 \mu\text{m}$. Since V_{110}^{in} is proportional to the cavity size, the TM_{110} design frequency is 12 GHz (see Fig. 9b). With $q = 1 \text{ nC}$, $\beta = 1$ and $Q_L = 1000$ we get for the voltages

$$V_{110}^{in} \approx 464 \text{ [mV}/\mu\text{m}] \quad V_{110}^{out} \approx 9.9 \text{ [mV}/\mu\text{m}] \quad (25)$$

A complete monitor consists of two cavities separated in beam direction. The frequency shift due to the missing coupling in one plane is about 0.33%. The peak wake potential is about 20.7 V/pC for a bunch length of $50 \mu\text{m}$.

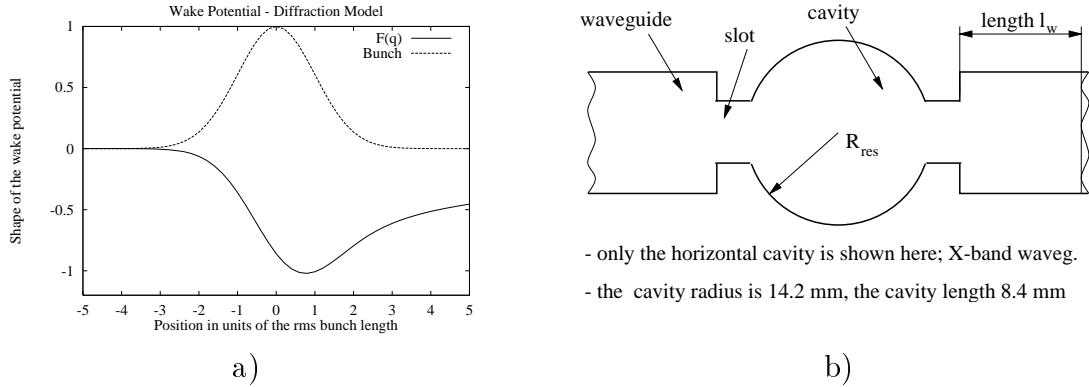


FIGURE 9. TTFL-FEL: a) Normalized wake potential; b) cavity, coupling to waveguides.

Design of a TM_{110} Cavity BPM

Cavities are narrowband devices and they have to be designed in the frequency domain. There are two main applications of cavity BPMs:

1. High resolution (in the nm-range), even for single bunches, and
2. Moderate resolution, but very low current (cw, about 1 nA).

TM₁₁₀ Frequency and Cavity Size

There is no ‘global’ optimal TM₁₁₀ frequency for each BPM application. A general rule is that it should be apart from the accelerating frequency in order to avoid interference of the position signals by leakage fields of the high rf power in the machine. In addition, f_{110} should be well below the frequency where the power density in the spectrum decreases by 3 dB. Otherwise, one has to take into account the bunch factor. This factor is about 1 for Gaussian bunches with $\sigma_z \leq 1$ mm and frequencies below 40 GHz. Beside that, the TM₀₁₀ frequency should not be a harmonic of the bunching frequency (multibunching).

TABLE 1. Arguments for a higher or a lower resonance frequency (fixed beam pipe radius).

Parameter	Higher frequency	Lower frequency	Remark
$f_{\text{TM}_{020}}$ above f_c	+	-	common-mode rejection
costs	(-)	(+)	electronics, vac.-feedthroughs
signal level	+	-	better: re-entrant (!)
reference, phase	(-)	(+)	

For optimum common-mode rejection the resonant frequency should be high (Eqn. (18)). The cavity radius is limited by the field distortion due to the beam pipe: for cavities that are too small the electric field is no longer linear/constant along the gap. A lower limit (practical experience) is that the cavity should be larger than three times the beam pipe radius. Hence, it is impossible to get a TM₀₂₀ frequency higher than the beam pipe cut-off without any distortion.

Concerning the costs, it is very important to chose the ‘right’ frequency, mainly because of the electronics (see Electronics section below) and existing hardware/software. Beside that, there are only a few vacuum feedthroughs on the market for frequencies above 10 GHz. Some arguments for a resonant frequency choice are listed in Table 1.

Influence of l/R_{res} on the TM₁₁₀ Signal

For the detection of *single bunches* the voltage induced in the cavity (Eqn. (14)) should be high. Since T_{tr} depends on the ratio $\xi = l/R_{\text{res}}$, the function $\sin^2 \xi/\xi$ has to be optimized, yielding $\xi_{opt} = 0.6086$ for a cavity without beam pipes.

In the case of multibunching, the shunt impedance has to be optimized according to Equation (15). Since Q_0 and Q_L cancel and only a coupling term remains, this leads to an optimization of the transit time factor. The resulting value for ξ_{opt} is 0.742. A more effective way to optimize the shunt impedance is to make the cavity re-entrant (‘nose-cones’). Such an optimization is usually done by using numerical codes.

Resonance Frequency for Multiple Bunches

Let us assume a cavity with $l = 0.742 \cdot R_{\text{res}}$ and $R_{\text{res}} = 3 \cdot R_o$, having two identical couplings of $\beta = 1$. Neglecting the ratio of the loss factors we get with equations

(12a), (7), and (19) for Q_L and the minimum resolution

$$Q_L \approx \sqrt{R_{\text{res}}} \cdot \sqrt{\kappa} \cdot \frac{11.45}{(1 + 2\beta)} \quad \delta x^{\text{min}} \approx \sqrt{R_{\text{res}}} \cdot \frac{0.227}{\sqrt{\kappa}} \quad (26)$$

Coupling by Antennae or by Waveguides

The signals excited in the cavity have to be coupled into an external circuit (see discussion in previous section). There are two strong arguments for having two ports per plane: for symmetry reasons and to realize a common-mode rejection (see below, subsection entitled “Other Signals and Resolution Limits”).

Type of Coupling

For frequencies below 10 GHz it makes sense to use antennae, mainly because of the size of waveguides in this frequency range (though these could be ridged). At higher frequencies it is both easier and more precise to use waveguides; antennae for such frequencies are so tiny that tolerances for length, thickness, angle, etc., are problematic.

Strong or Weak Coupling

A strong coupling leads to larger signals and is good for stabilizing the cavity (temperature drifts, etc.). But it lowers also Q_L (common-mode rejection, Equation (19)) and might lead to field distortion.

For the design it is important to determine the *coupling factor* of each port and to estimate the resulting *frequency changes*. The *perturbation method* can be used to predict the frequency change due to an antenna inserted in the cavity (Fig. 2c). First, a cavity is excited at its resonant frequency. A small object is then introduced, and the resulting frequency change is of the order of the volume ratio of the cavity and the object. In another theory by Bethe, the fields of small coupling holes are replaced by equivalent dipoles (\mathbf{M}_m and \mathbf{E}_e in Figure 2b and 2d). For more details of both methods the reader is referred to [5]. Another approach discussed below (see the “Numerical Methods” section) follows a method described in [22].

Number of Cavities

Both TM_{110} polarizations have to be measured to obtain the displacements in x and y, respectively. Single cavities are compact devices, and the distortion to the beam is smaller. A major problem is that of symmetry: the tuning and the coupling of one polarization effects also the other polarization. This additional asymmetry leads to a lower isolation between both polarizations (‘cross-talk’). By using two cavities separated in beam direction, the unwanted polarization in each

of the cavities can be detuned and/or additionally damped (thus reducing the wakefields and the decay time). The beam pipe acts as a waveguide below cut-off, the attenuation of a TM_{01} wave at a position z_0 can be calculated using Equation 2 and $\lambda_c = 2.613 \cdot R_{\text{res}}$. Table 2 summarizes some of the arguments for both structures.

TABLE 2. Comparison: two cavities versus a single cavity

Parameter	Single cavity	Two cavities
Isolation/Cross talk	about 25 dB	more than 40 dB
Tuning and Coupling	complex, less space	individual, better for symmetry
Coupling	possible, but less space	independent for both planes
Wakefields, losses	smaller	higher
Space	short	long
Fabrication and costs	easy/lower	complex/higher
Temperature stabilization	easier	complex, but independent

Numerical Methods

The equations for the calculation of fundamental cavity parameters are true only for cavities without any perturbation. Electromagnetic computer-aided design (ECAD) is needed, e.g., to estimate the impact of re-entrant parts, of beam pipe holes or of bellows on the resonance frequency. 2D codes such as SUPERFISH or URMEL/MAFIA-2D are good enough for the first step, since most of the structures have an axis symmetry. In the case of azimuthal asymmetries, 3D codes such as MAFIA [24] are needed.

An example for the latter is the insertion of waveguides or antennae for coupling purposes. In a method by Slater [22] the waveguide coupled to the cavity is shortened at a position l_w (Fig. 9b), thus forming a second resonator. This can be done for many positions l_w , and the resulting resonance frequencies of these systems of coupled resonators can be used to determine the external Q-value as well as the resonant frequency. This method is very useful for the numerical calculation of both quantities [11]. Besides these calculations in the frequency domain, the wake potentials and the total loss factor can be calculated in the time domain.

Mechanics, Fabrication, and Environment

Fabrication

Circular cavities can be built very precisely by turning. Most of the cavities used in particle accelerators are made of OFHC copper and their parts are brazed. In addition, aluminum and stainless steel were used for special applications [12]. For the cavities in Example 3, electro-discharge machining (EDM) was used to

realize the waveguides and the coupling to the cavity. Stainless steel/copper/water interfaces should be avoided because of electrolytic erosion.

Since f_{110} depends mainly on the cavity radius, the effect of temperature changes on the resonance frequency scales roughly with the expansion coefficient α of the material: $\Delta f_{110} = f_{110} \cdot \alpha$. Close dimensional tolerances of less than 0.02% are unavoidable for the cavity radius. Every reduction in azimuthal symmetry leads to an unwanted coupling between both polarizations in the cavity (cross-talk). A major problem is therefore to maintain the symmetry even after brazing or welding. The isolation is often reduced to about 25 dB, whereas it reaches about 35 dB for ‘ideal’ cavities. All internal cavity surfaces may be ‘polished’ if necessary.

Sometimes it is impossible to use standard rf components because of the special vacuum requirements in particle accelerators (10^{-9} Torr), and vacuum windows or special feedthroughs (e.g., by KAMAN Corp. or KYOCERA) are required. These feedthroughs can be used to develop special coax-to-waveguide adaptors.

Cryogenic Environment

A cryogenic environment has a strong impact on the design and the required reliability of beam instrumentation. Since operation at low temperatures is best achieved inside evacuated vessels, access to the beam pipe is quite difficult and maintenance requires long time scales. *Heat losses* should be kept to a minimum.

Cool-down causes a *shrinkage* of the cavity and changes the Q-values (*conductivity*). Since active tuning systems are very expensive, the design frequency should be reached after each cool-down within a certain bandwidth. Many materials most commonly used are not appropriate. Often special procedures are required to get ‘clean’ surfaces, since extraneous particles may affect, for example, high-Q superconducting accelerating cavities. Finally, special *rf feedthroughs* and cables are required to work reliably even at cryogenic temperatures.

Example 4: Cold monitors in the TESLA Test Facility Linac (TTFL)

Single circular cavities were built for steering correction at all superconducting quadrupoles, mainly because of the desired resolution, 10 μm in a cryogenic environment, and limited longitudinal space. The cavities are made of stainless steel to measure the position of single bunches at 1 μs spacing. A major problem in the mechanical design was to avoid asymmetries caused by welding. No active tuning system was allowed for this monitor.

Electronics

In most applications the resonance frequency is much higher than 1 GHz; consequently, rf-processing techniques are needed for signal detection. It is beyond

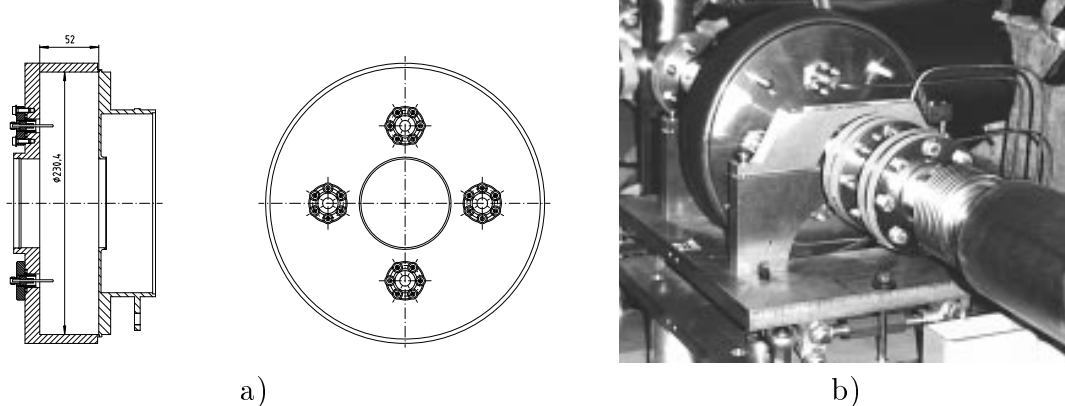


FIGURE 10. a) Design of the cold TTFL-monitors; b) warm monitor installed in the TTFL.

the scope of this paper to review all existing electronics used for cavity BPMs, or to discuss the rf electronics in detail. But this fact leads to some general remarks since it results in a more complex R&D than for other (low-frequency) BPMs.

Often the electronics design depends on the availability of components — an additional argument for selecting the ‘right’ frequency. Some commercially used frequency bands are at 900 MHz, at 1.9 GHz (PCS), and around 11 GHz (TV-sat, DBS). Components developed for these applications are cheap and ‘off the shelf’ (COTS). Otherwise more sophisticated design tools are needed for the development of individual circuits, for which special care has to be taken in terms of shielding, reflections, etc.

Synchronous Demodulation

The signal coupled out of the cavity decays with the time constant τ_r and can be treated as an amplitude modulation of the TM_{110} resonance. Therefore, most of the electronics developed for a cavity BPM employ the superheterodyne receiving technique: the signal is demodulated by mixing it down to an *intermediate frequency* (IF) within one or more stages. A special case is the *homodyne receiver*, having an IF-frequency of $f_{IF} = 0$ and yielding the TM_{110} envelope. The phase between the reference signal and the TM_{110} signal has to be adjusted and stabilized. Sometimes *I/Q-mixers* are used [12], where the signals are mixed in-phase and in-phase-quadrature. This results in a coordinate system in which the vector of the output signals I and Q rotates with the IF frequency.

The dynamic range of a receiver is given by the maximum input signal which is amplified or mixed without distortion, and the noise. Signals of less than 10^{-19} W were detected at MAMI [7] by using a phase-sensitive synchronous demodulation scheme (lock-in amplifier at 100 kHz).

Reference Signal

A reference signal is needed for the normalization as well as for getting the starting phase of the resonating field. The latter gives the sign of the displacement: when the beam is on the right, the system can be set up to give positive video polarity.

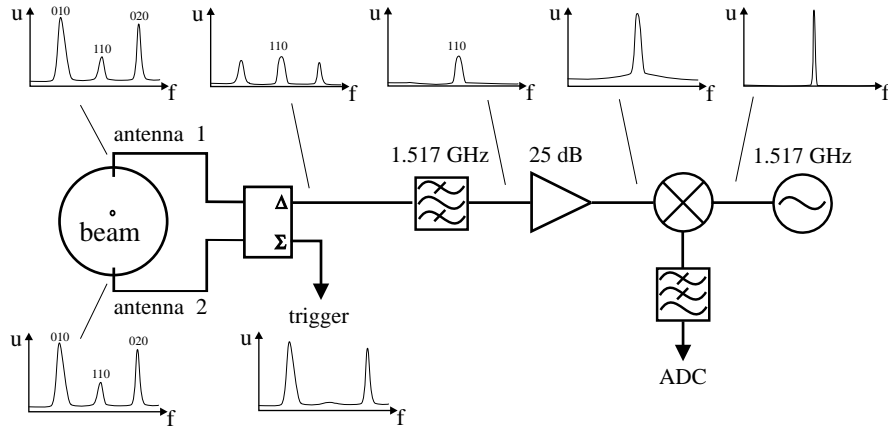


FIGURE 11. Block diagram of the homodyne receiver built for the detection of the beam-excited vertical TM_{110} polarization (TTFL-monitors, Example 4). The mixer is realized as an I/Q-mixer.

The signal changes the phase by 180° when the beam moves to the left, and for a centered beam it becomes zero. The phase difference relative to an external reference has to be measured approximately, however, at higher frequencies even this is not straightforward.

In many resonant monitors an additional circular cavity is used, excited in the TM_{010} mode. This cavity measures the bunch charge and yields a phase reference. Often its TM_{010} frequency is close to f_{110} in the BPM cavity. Another possibility is to use the TM_{010} signal of the BPM cavity. This signal — proportional to the bunch charge — is usually absorbed at the Σ -port of the field filter. In the third method, an external reference oscillator has to be phase-locked to the beam or to the timing system. Temperature drifts in long cables have to be corrected.

Measurements and Tests in the Lab

All cavity parameters — such as resonance frequencies, Q-values, coupling factors, and the effect of tuning systems — can be measured in the rf lab using a Vector Network Analyzer (VNA or generator). Usually, one can use the coupling ports of both polarizations, and no additional antenna is needed. The difference in the dielectric constants of vacuum and air causes a frequency offset of about 0.029 %.

The resolution and the precision of a BPM can be measured on a testbench by using a coaxial wire or an antenna. The cavity is excited by this antenna fed by a cw-source (VNA, Generator). For measuring the precision, the antenna is centered in one direction. Then the cavity is rotated by 180° , and the difference in the signal output yields the offset between the mechanical axis and the electrical center.

OTHER RESONANT STRUCTURES

Besides the simple circular cavity there are other resonant structures used in accelerators for beam position measurement (see, for example, [4]). One special example will be discussed below.

Higher Order Modes (HOM) in Accelerating Structures

Energy variations along the bunch train caused by wakefield effects lead to an increased projected emittance. This can be avoided in principle if the beam could be precisely centered in the accelerating structures to prevent the excitation of HOMs. Rather than relying on the BPMs and their good alignment with respect to the structures, a better approach to beam steering is to minimize the beam induced dipole signals directly [18]. Therefore, these signals occurring at frequencies higher than the accelerating mode³ have to be measured.

A position measurement resolution of 12 μm was demonstrated for the dipole mode spectrum of the SLC-structures (4.14 to 4.35 GHz) by using amplitude and phase detection. The uncertainty in the determination of the absolute center position was larger.⁴ Much better results were obtained during a test of a NLC prototype structure in the SLC linac. In these structures the lowest dipole mode band is Gaussianly detuned. Additional damping is provided by coupling the cells to four manifolds that run along the structure. These manifolds permit the measurement of the beam-induced dipole mode signals that originate throughout the structure. By these means it seems possible to realize an in situ straightness measurement of the structure.

CONCLUSIONS AND SUMMARY

Cavity BPMs offer many advantages, but they also have shortcomings:

- They provide very high transfer impedance (some $\text{k}\Omega$) and high sensitivity, but also impose a large effect on the beam (wakefields, impedances).
- They offer good linearity over a wide position range and enable beam position measurement with a single output.
- The amplitude of the fundamental mode (the TM_{110} for rectangular and the TM_{010} for circular cavities) is proportional to the bunch charge or the current.
- The use of cavity BPMs saves longitudinal space compared to striplines, but costs transverse space.

3. For the properties of periodic structures, the reader is referred to [6].

4. Horizontal and vertical polarizations could not be separated; the couplers introduce asymmetries and the detected signals are a superposition from several structures.

Table 3 summarizes some principle arguments concerning the *cavity shape*. The signal levels are nearly the same for rectangular and for circular structures depending on the design.

TABLE 3. Arguments for the choice of the cavity shape.

Parameter	Circular Cavity	Rectangular Cavity	Remark
Fabrication	easy (turning)	standard waveguide	
Costs	low	moderate	
Precision	very high	moderate	welding, brazing
Tolerances	radius	waveguide length	most sens. parameter
Cooling	easy (copper tubes)	more complex	because of shape

Table 4 summarizes some of the existing cavities used for position detection; it is not a complete list of all resonant monitors.

TABLE 4. Existing cavities (*) and new monitors (o), beam-tested or under development.

Lab	Machine	Type	f_{110}	Q-values		Resolution	Excitation (min.)	
			[GHz]	Q_0	Q_L	[μm]	current (cw)	charge
Mainz	MAMI *	cyl.	2.449	9300	6100	50	1 nA	-
SLAC	SLC *	rect.	2.856			10	100 μA	-
CERN	CLIC o	cyl.	30.000			0.1	-	1 nC
TJNAF	CEBAF o	cyl.	1.497		3500	10	1 nA	-
DESY	TTFL o	cyl.	1.517		1000	10	5 mA	8 nC
KEK	JLC o	cyl.	5.712		140	0.025	-	(1 nC)
Mainz	MAMI o	cyl.	9.795	7500	2500	(2)	1 μA	-
DESY	FEL o	cyl.	12.000		1000	10	-	1 nC
BINP	VLEPP o	cyl.	14.000			0.010	-	(?)

ACKNOWLEDGMENTS

I would like to thank all people who helped me in the preparation of this talk. Special thanks are extended to T. Shintake and H. Euteneuer for sending very useful information about their work at the FFTB and at Mainz.

REFERENCES

1. Chin, Y. H., *User's Guide for ABCI Version 8.7*, CERN SL/94-02 AP, 1994.
2. Balakin, V., et al., "Beam Position Monitor with Nanometer Resolution for Linear Collider," in *Proceedings of the European Particle Accelerator Conference (EPAC94)*, London, 1994, pp. 1539–1541.
3. Bane, K. L., M. Sands, "Wakefields of Very Short Bunches in an Accelerating Cavity," SLAC-PUB-4441, Nov. 1987.

4. Bossart, R., "Microwave Beam Position Monitor Using a Reentrant Coaxial Cavity," CLIC-Note 174, CERN, 1992.
5. Collins, R. E., "Field Theory of Guided Waves," New York: IEEE Press (1991).
6. Dome, G., "RF Theory," presented at the CERN Accelerator School, Exeter College, Oxford, 1991; also published as CERN 92-03, p. 1-96.
7. Euteneuer, H., Universitaet Mainz, private communication.
8. Doerk, T., Institut f. Kernphysik, Uni Mainz, Diploma Thesis, 1996.
9. Farkas, Z. D., et al., "Precision Energy Measurement Technique," SLAC-PUB-1970, 1977.
10. McKeown, J., "Beam Position Monitor Using a Single Cavity," in *IEEE Transactions on Nuclear Science*, Vol. 26, No. 3, 1979, pp. 3423-3425.
11. Kroll, N. M. and D. U. L. Yu, "Computer Determinations of the External Q and Resonant Frequency of Waveguide Loaded Cavities," *Part. Acc.* 34, pp. 231-250 (1990).
12. Lorenz, R., et al., "First Operating Experiences of Beam Position Monitors in the TESLA Test Facility Linac," contributed to the 1997 Particle Accelerator Conference (PAC97), Vancouver, May 1997.
13. Lorenz, R., et al., "Beam Position Measurement Inside the FEL-Undulator at the TESLA Test Facility Linac," presented at the DIPAC97, Frascati, 1997.
14. Mazaheri, G., et al., "Development of Nanometer Resolution C-Band Radio Frequency Beam Position Monitors in the Final Focus Test Beam," these proceedings.
15. Piller, M., et al., "1 nA Beam Position Monitor," unpublished manuscript.
16. Rossbach, J., "Options and Trade-Offs in Linear Collider Design," in *Proceedings of the 1995 Particle Accelerator Conference (PAC95)*, pp. 611-615 (1995).
17. Schnell, W., "Common-mode rejection in resonant microwave position monitors for linear colliders," CERN, CLIC Note 70 (1988).
18. Seidel, M., "Studies of beam Induced Dipole-Mode Signals in Accelerating Structures at the SLC," SLAC-PUB-7557, June 1997.
19. Shafer, R., "Beam Position Monitoring," in *AIP Conf. Proc. 212*, pp. 26-58 (1989).
20. Sladen, J. P. H., et al., "Measurement of the Precision of a CLIC Beam Position Monitor," CLIC Note 189, CERN (1993).
21. Sladen, J. P. H., et al., "CLIC Beam Position Monitor Tests," in *Proceedings of EPAC96* (conference held in Sitges, Barcelona, Spain, 10-14 June 1996), pp. 1609-1611 (1996).
22. Slater, J. C., *Microwave Electronics*, Bell Telephone Laboratory Series, New York: Van Nostrand (1950).
23. *A VUV Free Electron Laser at the TESLA Test Facility Linac — Conceptual Design Report*, DESY Hamburg, TESLA-FEL 95-03 (1995).
24. Weiland, T., "On the Numerical Solution of Maxwell's Equations and Applications in the Field of Accelerator Physics," *Part. Acc.* 15, pp. 245-292 (1984).
25. Vogel, V., "BPM for VLEPP," in *Proceedings of the ECFA-workshop on e^+e^- Linear Colliders (LC 92)*, workshop held in Garmisch-Partenkirchen, 1992.